Correction (29 October 2013): A label in fig. S2A was corrected.

www.sciencemag.org/cgi/content/full/science.1243417/DC1

Supplementary Materials for

Circadian Clock NAD$^+$ Cycle Drives Mitochondrial Oxidative Metabolism in Mice

Clara Bien Peek,* Alison H. Affinati,* Kathryn Moynihan Ramsey, Hsin-Yu Kuo, Wei Yu, Laura A. Sena, Olga Ilkayeva, Biliana Marcheva, Yumiko Kobayashi, Chiaki Omura, Daniel C. Levine, David J. Bacsik, David Gius, Christopher B. Newgard, Eric Goetzman, Navdeep S. Chandel, John M. Denu, Milan Mrksich, Joseph Bass†

*These authors contributed equally to this work.
†Corresponding author. E-mail: j-bass@northwestern.edu

Published 19 September 2013 on *Science* Express
DOI: 10.1126/science.1243417

This PDF file includes:

Supporting Descriptions:

Supporting Description 1

In order for a biological process to be classified as circadian, it must display an endogenous oscillation of ~24 hrs in the absence of entraining factors. Experimentally, the rhythm must repeat itself for at least two ~24 hr cycles and persist in the absence of external cues (e.g. light or feeding cues). Thus, to determine whether FAO displays circadian oscillations independent of entraining cues caused by either feeding rhythms or the light-dark cycle, we collected tissues for FAO measurements every 4 hrs over the course of 48 hrs in mice that had been both fasted and maintained in constant darkness (Fig. 1A). Prior to sacrifice at each circadian time point, mice were fasted for 18 hrs, a length of time determined to induce maximal FAO (Fig. S2C) and sirtuin expression in liver (*17*). This length of fasting also minimizes potentially confounding effects of behaviorally-generated rhythms of fasting and feeding.

Supporting Description 2

We also compared oxygen consumption rates (OCR) in isolated mitochondria from wild-type mouse liver in response to either palmitoyl-carnitine plus malate or pyruvate plus malate at two different times of day (Fig. S4C). Compared to ZT0, we observed a relative decrease in OCR in response to pyruvate and malate at ZT12 during

the transition from the rest to active period in fasted mice (Fig. S4C), suggesting an intrinsic difference in the relative respiration from oxidative versus glycolytic-derived substrate at the two major behavioral and nutrient state transitions (ZT0 and ZT12). Further, since all mice had previously been fasted, this difference does not appear to be the result of differences in the feeding cycle.

Supporting Description 3

While NMN injection led to a complete rescue of uncoupled (FCCP-treated) respiration in isolated mitochondria, ADP-stimulated respiration was not completely increased to WT amounts (Fig. 2B), suggesting that circadian mutants possess both an NAD^+-dependent defect in oxidative fuel entry into the electron transport chain, as well as an NAD^+-independent defect in coupled respiration.

Supplementary Figure Legends:

Fig. S1 Circadian clock control of MEF metabolism. Relative amounts of NAD^+, FAO, mitochondrial ATP (in galactose-containing media), and lactate (in glucose-containing media) in *Bmal1*$^{-/-}$ and *Cry1*$^{-/-}$/*Cry2*$^{-/-}$ MEFs compared to controls (n=6). *p<0.05, **p<0.01, ***p<0.001 for Student's two-tailed t-test comparing control and mutant averages. Data are represented as average ± SEM.

Fig. S2 Cell-autonomous circadian control of FAO in liver. (A) Relative NAD^+ and FAO in liver from fasted liver-specific *Bmal1*$^{-/-}$ mice and littermate controls collected at ZT0 (n=4–7). **(B)** Blood glucose in WT and *Bmal1*$^{-/-}$ mice at ZT12 following an 18 hr fast (n=6). **(C)** FAO at ZT12 in WT mice following increasing lengths of fasting. **p<0.01,

***p<0.001 for Student's two-tailed t-test comparing single time points between WT and mutant averages. Data are represented as average ± SEM.

Fig. S3 Circadian regulation of intrinsic mitochondrial function. (A) Mitochondrial NAD^+ in liver of fasted WT mice maintained in constant darkness and collected every 4 hrs for 24 hrs. Shading indicates where light and dark periods would normally occur in 12:12 light-dark conditions (n=3 per time point). **(B-C)** Relative oxygen consumption rates in isolated liver mitochondria from fasted WT and *Bmal1*$^{-/-}$ mice at ZT0 **(B)** or ZT12 **(C)** following FCCP treatment in the presence of indicated substrates (n=3-4). **(D)** Relative liver mitochondrial NAD^+ in fasted WT and *Bmal1*$^{-/-}$ mice following injection with either saline or NMN 12 hrs prior to ZT0 collection (n=4). *p<0.05, **p<0.01, ***p<0.001 for Student's two-tailed t-test comparing single time points between WT and mutant averages. Data are represented as average ± SEM.

Fig. S4 Circadian control of fatty acid oxidation in C2C12 cells. (A) Relative NAD^+ in synchronized C2C12 cells (n=3). **(B)** Relative FAO and GO in synchronized C2C12 cells (n=1). **(C)** Ratio of OCR in the presence of palmitoyl-carnitine to pyruvate and malate in WT isolated liver mitochondria collected at ZT0 or ZT12 (n=5). **p<0.01 for Student's two-tailed t-test comparing WT averages at each time point. Data are represented as average ± SEM.

Fig. S5 Increased glycolytic gene expression in circadian mutants. (A) Relative mRNA expression of *liver pyruvate kinase (L-Pk)* in liver of 18-hr fasted WT mice

maintained in constant darkness and collected every 4 hrs for 48 hrs. FAO rhythm is shown for reference (n=4). **(B)** Relative mRNA expression of *pyruvate dehydrogenase kinase 1* (*Pdk1*), *lactate dehydrogenase A* (*Ldha*), and *phosphofructokinase 1* (*Pfk1*) in *Bmal1*$^{-/-}$ and *Cry1*$^{-/-}$/*Cry2*$^{-/-}$ MEFs compared to controls. (**C**) Relative mRNA expression of *Pdk1*, *Ldha*, and *L-Pk* in *Bmal1*$^{-/-}$ mutant mouse liver compared to controls at ZT0 (n=9–11) and ZT12 (n=3-4). **(D)** Relative mRNA expression of glycolytic genes in liver-specific *Nampt*$^{-/-}$ liver (n=5-6). **(E)** Relative NAD^+ and lactate production in WT MEFs treated with FK866 (n=2-3). *p<0.05, **p<0.01, ***p<0.001 for Student's two-tailed t-test comparing single time points between WT and mutant averages. Data are represented as average ± SEM.

Fig. S6 Normal mitochondrial biogenesis in circadian mutants. (A) Ratio of mitochondrial to nuclear DNA in liver from fasted WT and *Bmal1*$^{-/-}$ animals at ZT0 and ZT12 (n=9–11). **(B)** Immunoprecipitated PGC1α from WT and *Bmal1*$^{-/-}$ fasted liver at ZT0 immunoblotted for acetylated-lysine and PGC1α. **(C-D)** Relative mRNA expression of *Pparα* **(C)** and genes involved in mitochondrial biogenesis **(D)** in liver from fasted WT and *Bmal1*$^{-/-}$ animals at ZT0 and ZT12 (n=9–11). *p<0.05, **p<0.01, ***p<0.001 for Student's two-tailed t-test comparing WT and mutant averages at either ZT0 or ZT12. Data are represented at average ± SEM.

Fig. S7 Circadian control of SIRT3 activity. (A) Relative LCAD activity in liver mitochondrial extracts from fasted WT and *Bmal1*$^{-/-}$ animals at ZT0 (n=6). **(B)** Relative OTC activity in liver mitochondria from fasted WT mice maintained in constant darkness

and sacrificed every 4 hrs for 48 hrs (n=4). **(C)** OCR in mitochondria isolated from liver of fasted WT and *Sirt3*$^{-/-}$ mice in the presence of palmitoyl-carnitine following FCCP treatment at ZT0 (n=3). **p<0.01, ***p<0.001 for Student's two-tailed t-test comparing single time points between WT and mutant averages. Data are represented as average ± SEM.

Fig. S8 Normal SIRT3 protein expression in circadian mutants. (A) SIRT3 protein abundance in liver from fasted WT mice maintained in constant darkness and collected every 4 hrs for 48 hrs. COXIV immunoblotting was performed as a loading control. **(B)** SIRT3 and MCAD protein in liver mitochondria from fasted WT and *Bmal1*$^{-/-}$ animals at ZT0. COXIV immunoblotting was performed as a loading control (n=3). **(C)** SIRT3 and β-actin protein in liver from fasted WT and *Bmal1*$^{-/-}$ mice collected at ZT0 following injection with NMN for either 12 hr (top) or 10 consecutive days (bottom) prior to collection.

Fig. S9 Circadian control of SIRT3 activity is independent of redox ratio and nicotinamide levels. (A) NAD^+/NADH ratio in WT and *Bmal1*$^{-/-}$ MEFs (n=6). **(B)** *In vitro* deacetylase activity of recombinant SIRT3 on acetylated SIRT3-selective target peptide in the presence of constant NAD^+ and increasing concentrations of NADH. **(C)** Nicotinamide (left) and acetyl-CoA (right) measurements in liver from fasted WT and *Bmal1*$^{-/-}$ mice at ZT0 (n=3-6). *p<0.05, **p<0.01 for Student's two-tailed t-test comparing single time points between WT and mutant averages. Data are represented as average ± SEM.

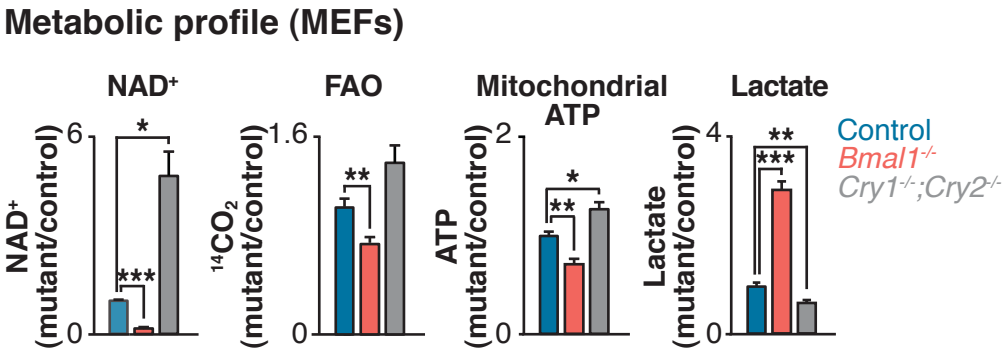
Metabolic profile (MEFs)
NAD+
FAO
Mitochondrial ATP
Lactate
NAD+ (mutant/control)
14CO2 (mutant/control)
ATP (mutant/control)
Lactate (mutant/control)
6
0
1.6
0
2
0
4
0
*
***
**
**
*
**
***
Control
Bmal1-/-
Cry1-/-;Cry2-/-

Figure S1

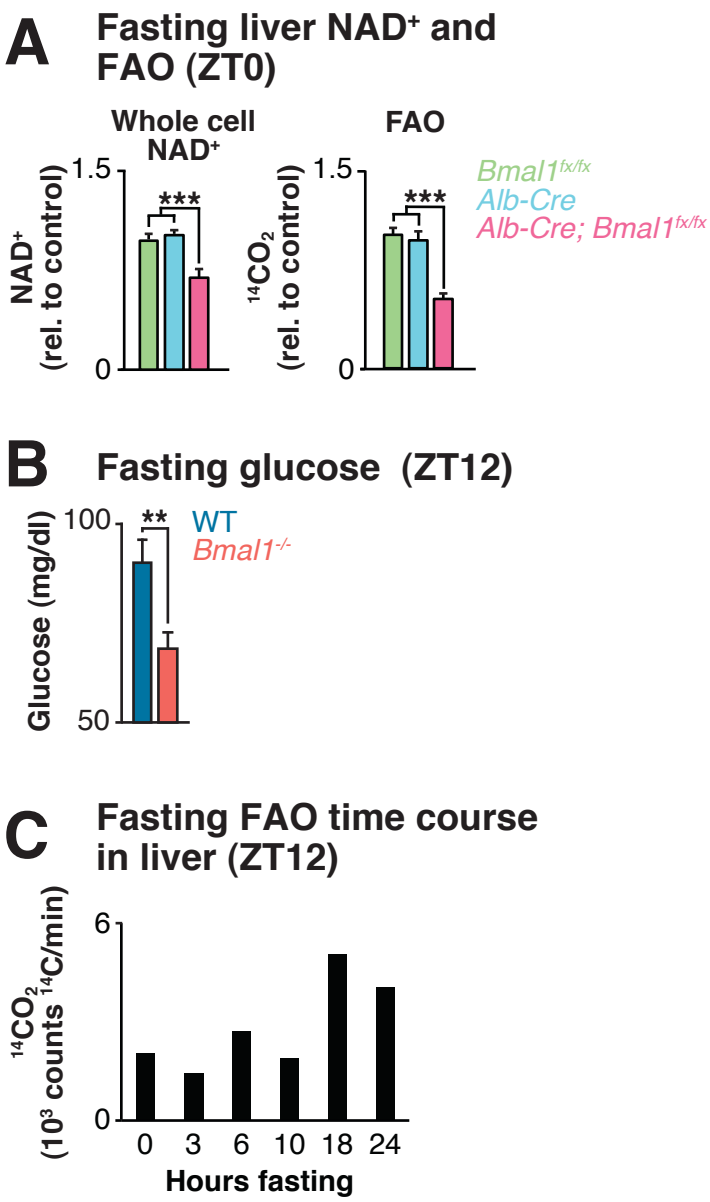
A
Fasting liver NAD+ and FAO (ZT0)
Whole cell NAD+
FAO
NAD+ (rel. to control)
14CO2 (rel. to control)
1.5
0
***
Bmal1fx/fx
Alb-Cre
Alb-Cre; Bmal1fx/fx
B
Fasting glucose (ZT12)
Glucose (mg/dl)
100
50
**
WT
Bmal1-/-
C
Fasting FAO time course in liver (ZT12)
14CO2 (10³ counts 14C/min)
6
0
0 3 6 10 18 24
Hours fasting

Figure S2

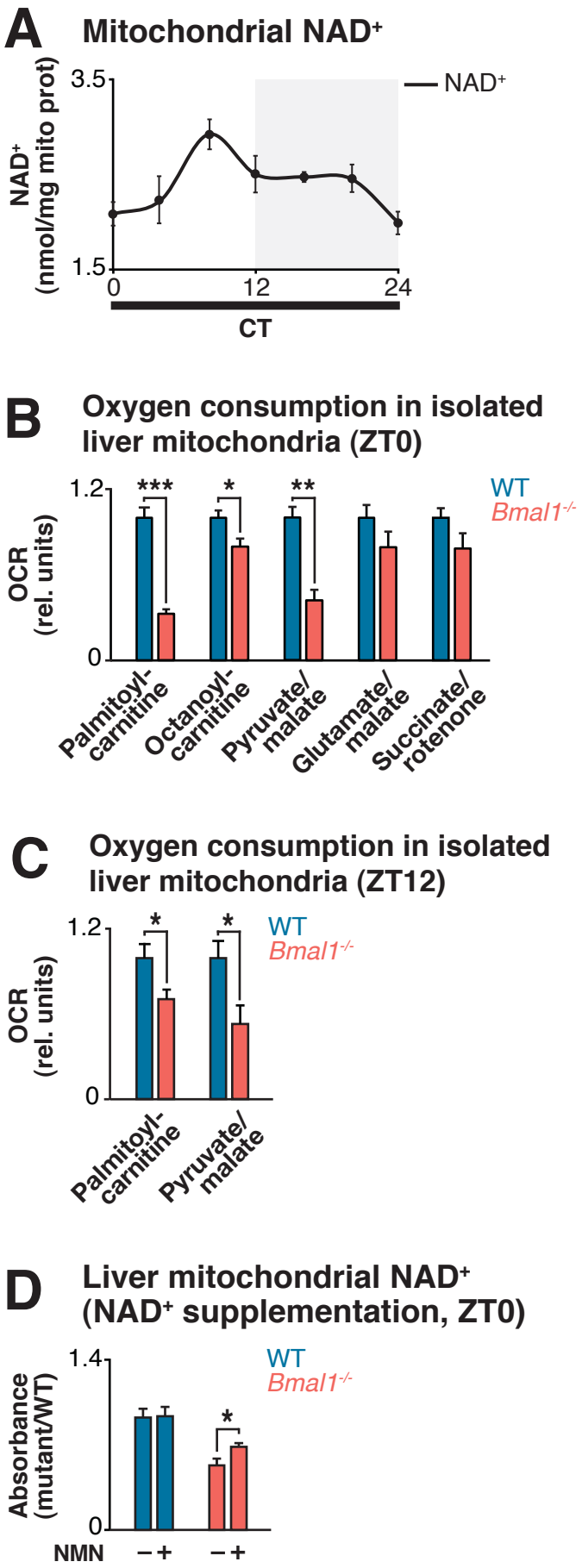
A
Mitochondrial NAD+
NAD+
(nmol/mg mito prot)
3.5
1.5
0
12
24
CT
NAD+
B
Oxygen consumption in isolated
liver mitochondria (ZT0)
OCR
(rel. units)
1.2
0
***
*
**
WT
Bmal1-/-
Palmitoyl-
carnitine
Octanoyl-
carnitine
Pyruvate/
malate
Glutamate/
malate
Succinate/
rotenone
C
Oxygen consumption in isolated
liver mitochondria (ZT12)
OCR
(rel. units)
1.2
0
*
*
WT
Bmal1-/-
Palmitoyl-
carnitine
Pyruvate/
malate
D
Liver mitochondrial NAD+
(NAD+ supplementation, ZT0)
Absorbance
(mutant/WT)
1.4
0
*
WT
Bmal1-/-
NMN
–
+
–
+

Figure S3

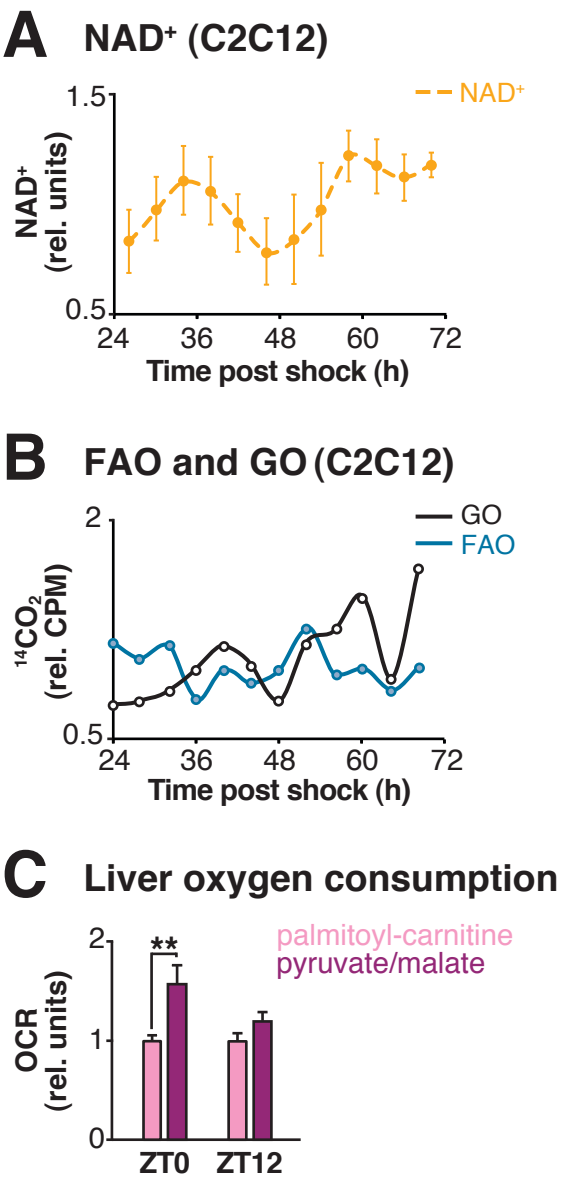
A
NAD+ (C2C12)
NAD+
1.5
0.5
NAD+ (rel. units)
24
36
48
60
72
Time post shock (h)
B
FAO and GO (C2C12)
GO
FAO
2
0.5
14CO2 (rel. CPM)
24
36
48
60
72
Time post shock (h)
C
Liver oxygen consumption
palmitoyl-carnitine
pyruvate/malate
**
2
1
0
OCR (rel. units)
ZT0
ZT12

Figure S4

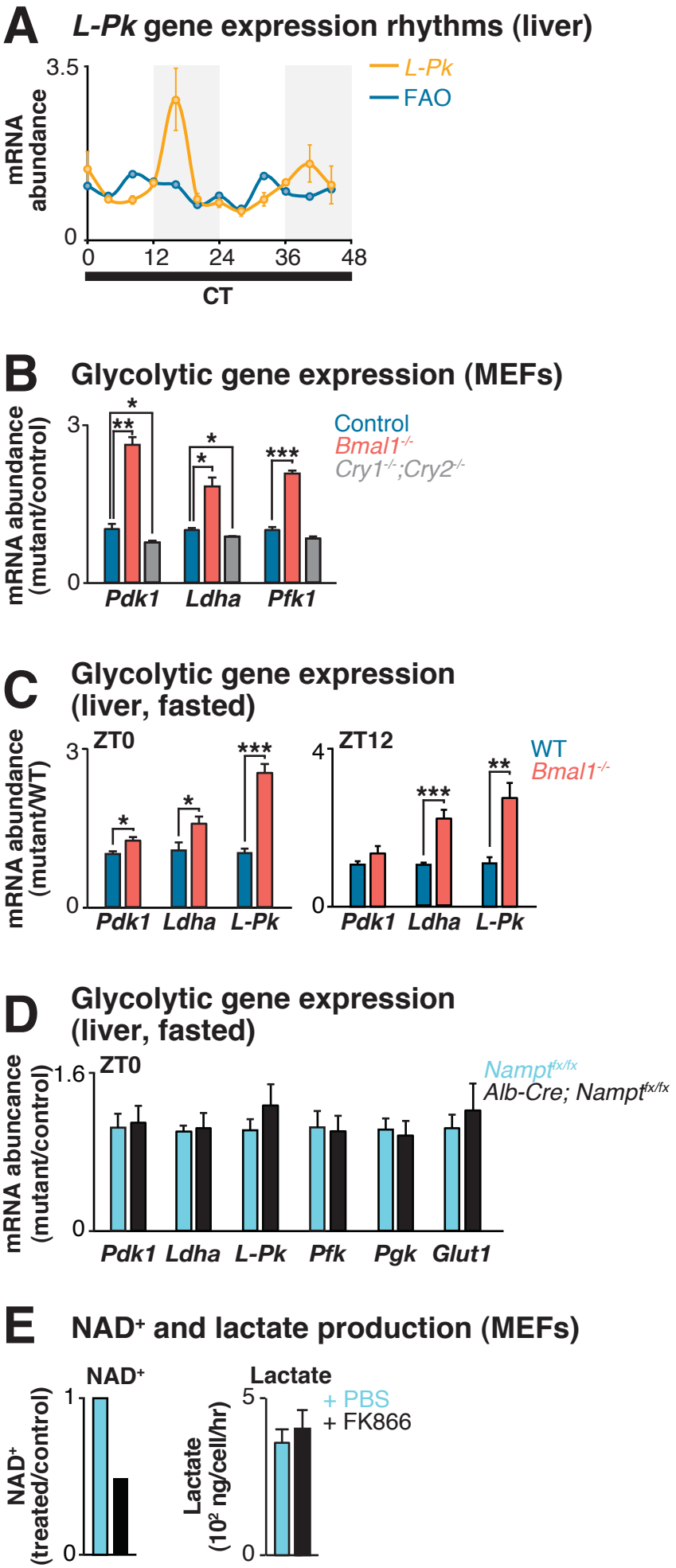
A
L-Pk gene expression rhythms (liver)
mRNA abundance
3.5
0
0
12
24
36
48
CT
L-Pk
FAO
B
Glycolytic gene expression (MEFs)
mRNA abundance (mutant/control)
3
0
Pdk1
Ldha
Pfk1
Control
Bmal1-/-
Cry1-/-;Cry2-/-
C
Glycolytic gene expression (liver, fasted)
mRNA abundance (mutant/WT)
ZT0
ZT12
3
4
0
Pdk1
Ldha
L-Pk
WT
Bmal1-/-
D
Glycolytic gene expression (liver, fasted)
mRNA abuncance (mutant/control)
ZT0
1.6
0
Pdk1
Ldha
L-Pk
Pfk
Pgk
Glut1
Nampt fx/fx
Alb-Cre; Nampt fx/fx
E
NAD+ and lactate production (MEFs)
NAD+ (treated/control)
NAD+
1
0
Lactate (10² ng/cell/hr)
Lactate
5
0
+ PBS
+ FK866

Figure S5

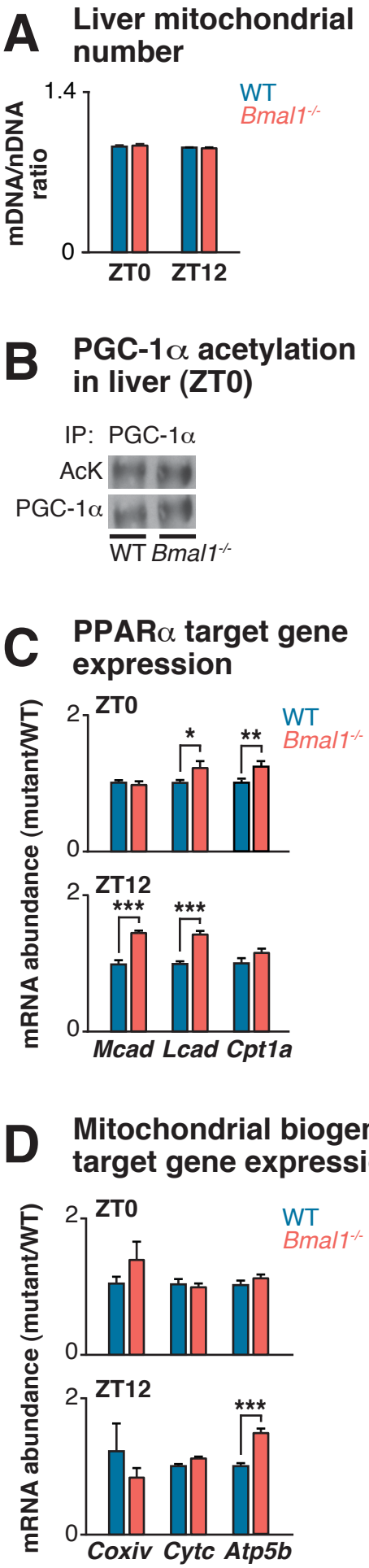
A
Liver mitochondrial number
mDNA/nDNA ratio
1.4
0
WT
Bmal1-/-
ZT0
ZT12
B
PGC-1α acetylation in liver (ZT0)
IP: PGC-1α
AcK
PGC-1α
WT Bmal1-/-
C
PPARα target gene expression
mRNA abundance (mutant/WT)
ZT0
ZT12
2
0
*
**
***
WT
Bmal1-/-
Mcad Lcad Cpt1a
D
Mitochondrial biogenesis target gene expression
mRNA abundance (mutant/WT)
ZT0
ZT12
***
WT
Bmal1-/-
Coxiv Cytc Atp5b

Figure S6

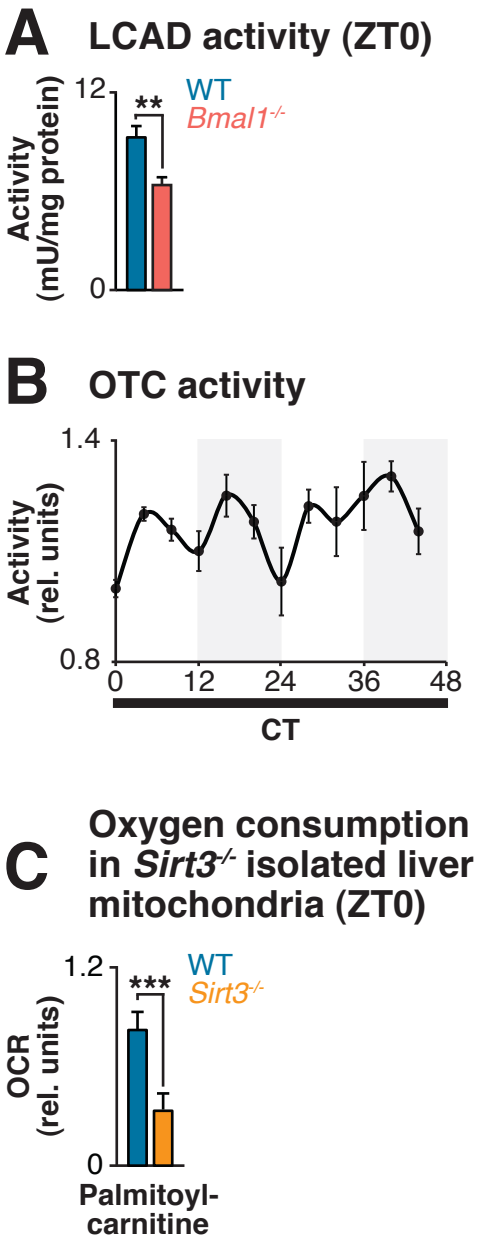
A
LCAD activity (ZT0)
Activity (mU/mg protein)
12
0
**
WT
Bmal1-/-
B
OTC activity
Activity (rel. units)
1.4
0.8
0
12
24
36
48
CT
C
Oxygen consumption in Sirt3-/- isolated liver mitochondria (ZT0)
OCR (rel. units)
1.2
0
***
WT
Sirt3-/-
Palmitoyl-carnitine

Figure S7

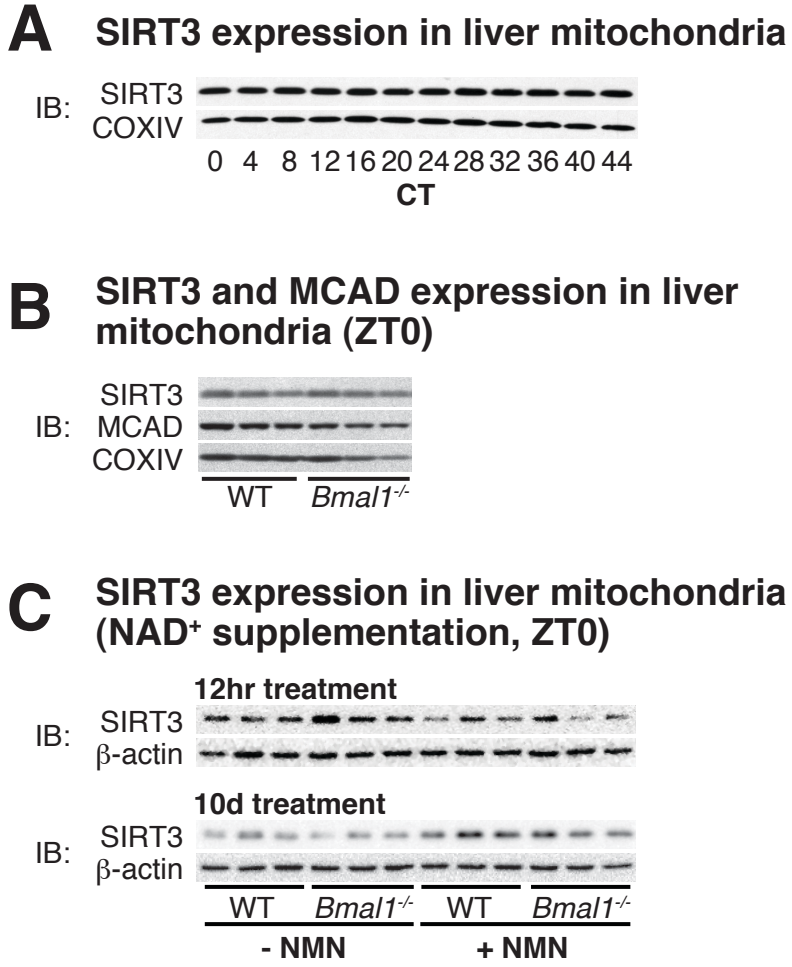
A
SIRT3 expression in liver mitochondria
IB:
SIRT3
COXIV
0 4 8 12 16 20 24 28 32 36 40 44
CT
B
SIRT3 and MCAD expression in liver mitochondria (ZT0)
IB:
SIRT3
MCAD
COXIV
WT
Bmal1-/-
C
SIRT3 expression in liver mitochondria (NAD+ supplementation, ZT0)
12hr treatment
IB:
SIRT3
β-actin
10d treatment
IB:
SIRT3
β-actin
WT
Bmal1-/-
WT
Bmal1-/-
- NMN
+ NMN

Figure S8

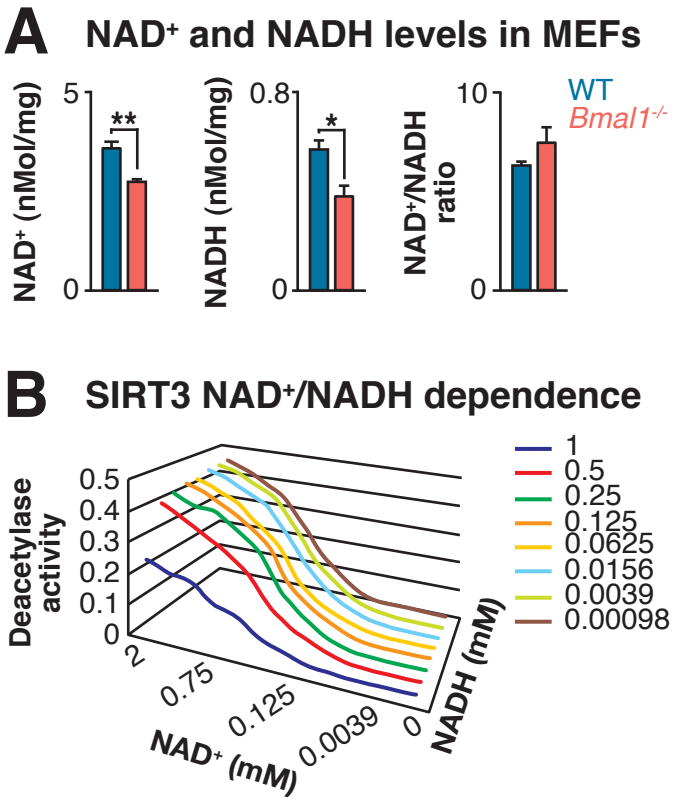
A
NAD+ and NADH levels in MEFs
NAD+ (nMol/mg)
5
0
**
NADH (nMol/mg)
0.8
0
*
NAD+/NADH ratio
10
0
WT
Bmal1-/-
B
SIRT3 NAD+/NADH dependence
Deacetylase activity
0.5
0.4
0.3
0.2
0.1
0
2
0.75
0.125
0.0039
0
NAD+ (mM)
NADH (mM)
1
0.5
0.25
0.125
0.0625
0.0156
0.0039
0.00098
C
Nicotinamide and acetyl-CoA levels in liver (ZT0)
Nicotinamide (μg/g tissue)
50
0
Acetyl-CoA (10² pmol/mL)
15
0
WT
Bmal1-/-

Figure S9